Seventh International Conference on Construction in the 21st Century (CITC-VII)
"Challenges in Innovation, Integration and Collaboration in Construction & Engineering"
December 19-21, 2013, Bangkok, Thailand

Shear Capacity of Rectangular Industrial Duct Panel

K.S.Sivakumaran
Department of Civil Engineering, McMaster University, Hamilton, Ontario, Canada L8S 4L7
siva@mcmaster.ca

T. Thanga
Senior Structural Engineer, Hatch Ltd, Mississauga, Ontario, Canada, L5K 2R7
TThanga@hatch.ca

B. Halabiah
BAH Enterprises Inc., 1088 Kent Avenue, Oakville, Ontario, Canada, L6H 1Z6
bhalabieh@bahinc.ca

Abstract
The end panels of a large rectangular industrial duct experience significant internal pressures and considerable transverse shear at the support locations. Though the designers depend on the plate girder design methods, the structural dimensions and the arrangements, the loadings and the resulting behaviour of the such end panels are significantly different. Large aspect ratio of the end panels gives rise to multiple bands of tension fields and significant membrane action, whereas the plate girder web design is based on one tension field. In this investigation, a nonlinear finite element model was developed to simulate the behaviour of industrial duct end panel subjected to transverse shear and internal pressures. The model considered the geometric imperfections and constitutive relations for steels. Six scale independent dimensionless parameters that govern the behavior of such end panels were identified as $b/t\sqrt{F_y/E}$, Δ/t, σ_m/F_y, h/b, $V/[ht(Fy/\sqrt{3})]$, and δ/b, which were then used in an extensive parametric study, which primarily established the ultimate shear strength of end panels. It was concluded that the plate slenderness dominates the shear strength of stockier end panels, whereas, the aspect ratio and plate slenderness influence the shear strength of slender end panels. This paper proposes design aids for shear strength of thin end panels subjected to concurrent transverse shear and internal pressures.

Keywords
Thin Plate, Transverse Shear, Tension Field, Finite Element Analysis, Parametric Study, Design

1. Introduction

Many heavy industrial processes require transport of large amount of high pressure air or other gases through series of steel ducts, which are significantly large and in some ways are quite unique structures. The cross-sectional dimensions of such industrial rectangular ducts may be in the range of 5 m to 15 m. The positive or negative pressure inside the ducts may be in the range of 10 to 15 kPa. The vertical loads such as self weight, weight of insulation, dust load, etc., are transferred to the side walls as shear (which act as web) and then to the supports. Thus, the plate panels of the side walls adjacent to the support legs are subjected to large shear loads as well as internal pressure. This paper concerns with the behavior and design of industrial duct end panels subjected to concurrent transverse shear and internal pressures.

2. Behaviour of Thin Plates Under Shear

Consider a thin end panel shown in Figure 1, having a width b, height h and thickness t. Such a panel subjected to shear stress τ experiences in-plane tensile and compressive stresses σ. This compressive stress σ whose magnitude is equal to the applied shear stress τ and acts at 45^o to the shear axis, can cause buckling of the plate when the applied shear stress τ reaches the shear buckling stress τ_{cr} given as $\tau_{cr} = k\,\pi^2\,E/[12(1-v^2)(b/t)^2]$ Where $E =$ elastic modulus , $v =$ Poisson`s ratio and $k =$ shear buckling coefficient. For simply supported plates $k = 5.35 + 4.0\,(b/h)^2$ and for clamped plates $k = 8.98 + 5.6\,(b/h)^2$. In these expressions, b is the width of shorter dimension of the long plate (Timoshenko and Gere, 1961). The buckling stress τ_{cr} increases as the plate slenderness (b/t) decreases, and the stocky plates may fail by yielding in shear at $\tau_y = F_y/\sqrt{3}$, where F_y is the tensile yield strength. The limiting plate slenderness (b/t) for the shear yielding can be obtained by equating τ_y to shear buckling stress τ_{cr}. The limiting (b/t) for a simply supported plate with material properties of elastic modulus $E = 200{,}000$ MPa and yield strength of $F_y = 350$ MPa and with the aspect ratio (b/h)$= 1$ will be 90. However, for the plate of a side wall of large industrial duct, the ratio of the stiffener spacing to the plate thickness (b/t) will be much higher and in the range of 125 to 350. Thus, the applied shear stress will cause elastic buckling. However, beyond buckling, the plate has the capacity to carry additional shear load because of stable tensile stresses may be generated in diagonal direction. Therefore, the plate can carry additional shear load until yielding occurs in the plate. This is referred to as tension-field action, and post-buckling strength. Based on extensive studies on the post buckling behavior of the web panels by Basler (1961), AISC (1963) first included the post buckling strength in addition to elastic buckling shear capacity in its specification. The ultimate shear strength for the slender web panel in the current AISC (2005) is given by; $V_u = 0.6F_y ht\left[[\tau_{cr}/(F_y/\sqrt{3})] + \left(1 - [\tau_{cr}/(F_y/\sqrt{3})]\right)/1.15\sqrt{1+(b/h)^2}\right]$. The first term within the bracket represents the relative contribution of the buckling strength V_{cr}. The second term in the bracket is the increase of the plate shear strength due to one band of uniform diagonal tension field across the web. The end panels of industrial rectangular ducts, whose aspect ratio (h/b) may be higher than 2, can develop several bands of tension fields across the length of the plate when subjected to uniform shear. Furthermore, the end panel between stiffeners is subjected to lateral pressure load, which produces bending stresses σ_b and the diaphragm stresses σ_m perpendicular to the stiffener direction, which are not accounted for in the above Vu expression (AISC, 2005). This investigation attempts to establish the impact of these factors on the shear strength of industrial duct end panels. Here, a finite element method based parametric study was conducted to investigate the issues.

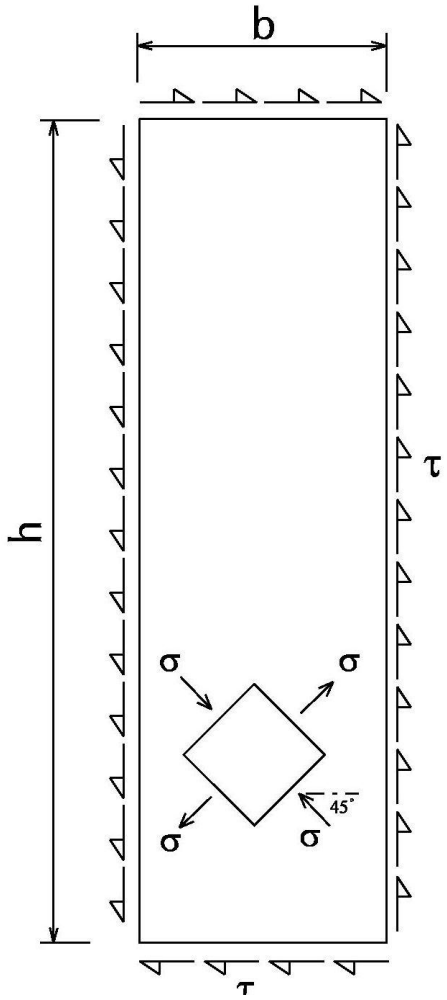

Figure 1: End Panel Subjected to Shear

3. The Finite Element Analysis Model for Industrial Duct End Panels

The finite element analysis method can be conveniently used to accurately trace the buckling behaviour of plate panels. In addition to obtaining their collapse modes, the finite element analysis will give the

deformations and stresses of a plate panel subjected to shear loads and pressure loads. A schematic of duct side panel selected for the parametric study presented in this paper is shown Figure 2. The duct side panel consists of a plate panel bounded by two adjacent stiffeners and the corner angles at its top and bottom. Typical angle L76X76X7.9 (3X3X5/16) and stiffener W200x27 (W8X18) were selected for this study. To simulate the behaviour of the plate panel subjected to shear, the finite element model was developed using a commercial general purpose nonlinear finite element program ADINA(2009). It has an extensive element library, material models and modeling capabilities appropriate for any nonlinear problems. In order to reach the convergence of the equilibrium of the nonlinear load-displacement path, a displacement control arc length iterative analysis method was used. A 4-node shall element based on updated Lagrangian formulation from ADINA element library was used to model the entire plate panel. This element can be used to model both thick and thin shell problems that require the Mindlin plate theory, and for large displacement and small strain problems. The available maximum of seven integration points through thickness were used for this analysis in order to capture the stress variation across the thickness, and thus to ensure accurate initiation and development of tension fields across the plate.

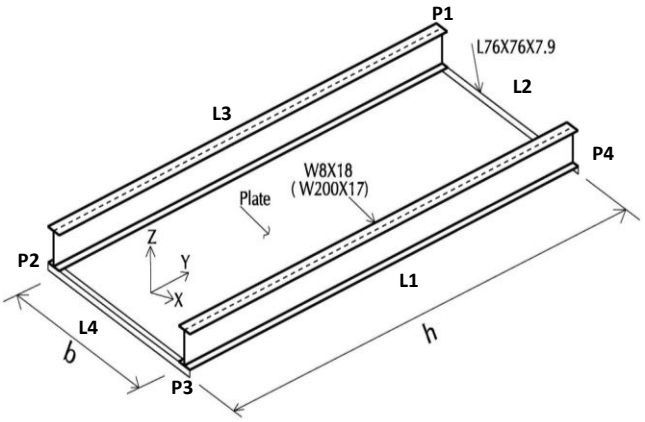

Figure 2: Schematic of Duct Side Panel

Loading and Boundary Conditions: It is very important that the boundaries must be incorporated realistically in a numerical simulation. The rotational stiffness of the longer edges of the plate panel (h dimension) depends on the rotational stiffness of the flange of the stiffeners connected to the plate. Therefore, the edge boundary condition of plate panel can be expected to be between fixed and simple. In order to represent the rotational stiffness of the flange of practical stiffeners, typical stiffener W200X27 (W8X18) was modeled along both longer edges of the plate panel. The transverse edges of the stiffeners, however, were not restrained against the rotation along the transverse direction. In large industrial duct side plate panels, adjacent to the supports transfer large amount of shear. At ultimate states, the horizontal components of tension fields cannot be anchored by the adjacent side panel that is outside of support rings as one support ring in industrial duct is allowed to slide toward the duct longitudinal axis. Also the panel on outside of the support has lesser shear load, thus no tension field to balance the horizontal components. Therefore, the translations of longer edges along the transverse direction were not restrained. In addition, this translation of longer edges will be uniform as the plate is continuous on either side of the end panel under consideration. As shown in Figure 2, the $x-y$ plane coincides with the middle plane of the plate panel. The z-axis is perpendicular to the plate and originating from the centre of the plate panel. Let us take u_1, u_2, and u_3 as the translations along the x, y, and z directions, respectively and θ_1, θ_2, and θ_3 as the rotations about the x, y, and z directions, respectively. The edges of the plate panel are labeled L_1, L_2, L_3 and L_4 the four corners of the plate panel are marked as P_1, P_2, P_3 and P_4. In order to provide the rotational stiffness along the plate and flange juncture, the rotation about the y direction and the translation along the z direction were restrained along the edges L_1 and L_3. In order to simulate the uniform translation of longer edges due to continuous plate, the translation along the x direction were constrained to be the same along the edges L_1 and L_3. The translation in z direction was restrained along the all edges. The translation along x direction was restrained at the point P_1 while the translation along x and y directions were restrained at the point P_2 to avoid any rigid body rotation. To simulate shear loading, uniformly distributed line loads were applied along plate edges.

Initial Geometric Imperfections: Geometric imperfections such as out-of-flatness of the plate and camber or sweep of structural members exist in their unloaded condition. The behavior of plate panel subjected to in plane forces is affected by initial out-of-flatness. The magnitude and shape of initial geometric

imperfection play a significant role in the response behavior. In this study, a pattern consisting of a half sine wave in transverse direction and a series of half waves in the longitudinal direction was introduced as follows: $\Delta_{imp} = \Delta_o \sin(\pi x/b)(\pi y/b)$, where Δ_{imp}= initial geometric imperfection distribution, Δ_o= maximum amplitude of the initial geometric imperfection, b = width of the plate panel, h = height of the plate panel, x = coordinate in the transverse direction of the plate panel and y = coordinate in the longitudinal direction of the plate panel. The maximum permissible variation of out of flatness of a steel plate for fabrication related initial imperfections was given in Paik and Thayamballi (2003) as $\Delta o/t = 0.025\,[(b/t)\sqrt{Fy/E}]^2$. In a large industrial duct, the deflected shape of the plate panel subjected to transverse pressure load should be incorporated as the plate panel considered is subjected to in plane shear and transverse pressure load as well. The deflected shape of the long plate panel due to transverse pressure can be assumed to be cylindrical. The relation between the plate slenderness and the normalized deflection (Δ/t), when the top fibre yields due to lateral pressure, was established in another study (Thanga, et al., 2013). Therefore, the pattern of initial geometric imperfection assumed for this study was the summation of the cylindrical deformation due to lateral pressure and the double sine function of out of flatness. This pattern was mapped onto the finite element mesh to model industrial duct end panel.

Material Model: The idealized elastic-plastic-strain hardening tri-linear material model representing mild carbon steel was used to model the material constitutive behavior of the plate panel. The yield strength of 250MPa (F_y) and modulus of elasticity of 200000MPa (E) were used to define the material of the plate panel. This represents the most common structural steel for plates, ASTM A36. The nominal strain at yield, ε_y, is Fy/E or 0.00125 for A36 steel. The strain hardening can be anticipated at a strain of around 10 times the ε_y. A constant proportionality is also presumed in the strain hardening range. The accepted strain hardening modulus E_{st} for mild carbon steels is E/30. The minimum tensile strength, F_u, for A36 steel is 400MPa. The plate, stiffener sections and corner angles were assumed to be made by A36 steel for this study. The material models in ADINA (2009) are based on incremental theories in which the total strain increment is decomposed into an elastic strain increment and a plastic strain increment. An incremental plasticity model is formulated in terms of yield surface, flow rule and a hardening rule. The von Mises yield surface is used to specify the state of stresses corresponding to start of plastic flow. The von Mises yield surface assumes that yielding metal has the form of a cylinder in three dimensional principal stress space. The von Mises criterion uses the associated flow rule for the development of plastics stress-strain relations of metals. The associated flow is the plastic flow developed along the direction normal to yield surfaces. A hardening rule specifies the yield surface during plastic flow. In this study, the isotropic hardening rule was selected. In the isotropic hardening rule, the size of the yield surface changes uniformly in all directions as plastic straining occurs. The isotropic hardening rule is more suitable for a static nonlinear analysis of this plate panel subjected to shear.

Mesh density and Validation Study: In order to establish a suitable mesh density for this numerical study, a convergent study was performed. The dimensions of the plate subjected to uniform shear load are: b $= 1000mm$, $h = 1000mm$ and $t = 5mm$. The amplitude of the double sine function of out of flatness of the plate is 6.25mm. The investigation considered five identical plate models with different mesh densities. The density of the coarse mesh is 6x6, while the density of the finer mesh is 26x26. The percentage changes in ultimate strength of each model were compared as the mesh was being refined. The percentage change in ultimate strength between mesh density of 6x6 to 10x10, to 16x16, to 20x20 and to 26x26 were 7.4%, 3.0%, 2.2% and 1.1%, respectively. It can be noted here that a reasonable degree of accuracy can be attained with a coarser mesh density. Due to the severe nature of the material and geometric nonlinearities involved the plate panel subjected to shear, a very dense mesh of shell elements was desirable in order to trace the nonlinear equilibrium path into the unloading regime. Thus, mesh density 16x16 was selected. In Physical dimensions, each element size is approximately 62.5 mm x 62.5 mm. To validate the model, the model developed for the convergence study was first applied to a square plate subjected to uniform shear, for which theoretical buckling results (211 kN) exist. The applied shear and the out of plane deflection at the middle of the plate were obtained from the results of the analysis for

each time step. It is difficult to distinguish between the pre buckling and post-buckling response paths of an imperfect plate subjected to uniform shear. However various techniques have been developed in order to obtain buckling load from experimental and numerical results. In one of those techniques, two tangent lines are drawn from two points where the slope changes with maximum rate and the intersection of the two tangents gives the buckling load. The buckling load obtained from the analysis results was around 210kN which was in very close agreement to the theoretical results.

4. Parametric Study

Dimensionless Parameters: This section identifies the fundamental parameters that affect the behavior and the ultimate strength of the industrial duct end panel. Then dimensionless parameters that define the behavior and ultimate strength are derived which are then used in a parametric study. These dimensionless parameters should be independent of any scale and material characteristic. The fundamental parameters governing the side plate panel are the geometric parameters of plate panel $b =$ width of the side plate panel, $h =$ height of the side plate panel , $t =$ thickness of the plate , and the response parameters $\Delta =$ initial out-of-plane deflection and $\sigma_m =$ diaphragm stress. The loading parameter is the applied shear V. The output variable is selected as the in-plane drift δ. The material parameters are: $E =$ modulus of elasticity (or $G =$ elastic shear modulus) and $F_y =$ yield strength of the plate material. It should be noted here the Δ is the algebraic sum of magnitude of initial geometric imperfection Δ_o and the deflection Δ due to internal pressure. Using Buckingham Pi-theorem (Langhaar, 1951) the 9 fundamental parameters can be reduced to 6 dimensionless parameters. Without going into details, the dimensionless parameters that govern the behaviour, including the ultimate strength, of end panel plates are the plate slenderness $b/t\sqrt{(Fy/E)}$, the aspect ratio h/b, normalized shear $V/[ht(Fy/\sqrt{3})]$, normalized drift δ/b, normalized deflection Δ/t, and normalized diaphragm stress σ_m/Fy . In a previous study (Thanga, et al., 2013) on a strip of plate subjected lateral pressure load a relation between $b/t\sqrt{(Fy/E)}$, and the dimensionless load parameter $pE/(Fy)^2$ was established corresponding to top fibre yielding. Corresponding Δ/t, and the diaphragm stress σ_m/Fy were also established. Therefore, for a particular plate slenderness $b/t\sqrt{(Fy/E)}$, the Δ/t and σ_m/Fy are known quantities, and thus for the problem under consideration, the parameters $b/t\sqrt{(Fy/E)}$, and $(h)/b$ are the input parameters, normalized shear $V/[ht(Fy/\sqrt{3})]$ is the loading parameter and δ/b is the output parameter. Three different end plate panels were considered in order to verify the completeness and the scale independence of the dimensionless parameters identified above. The three plate panels had the same dimensionless parameters $b/t\sqrt{(Fy/E)}$, and h/b but with different scale. The actual dimensions on these plates are given in the insert of Figure 3. Corresponding dimensionless parameters Δ/t, and σ_m/Fy were applied for this analysis even though these would be constant for the plate panels with the same $b/t\sqrt{(Fy/E)}$.

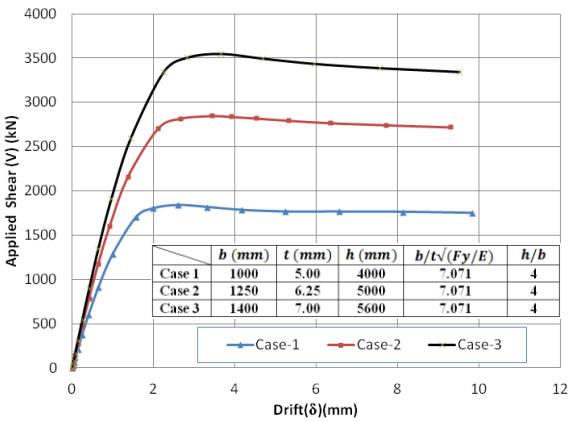

	b (mm)	t (mm)	h (mm)	$b/t\sqrt{(Fy/E)}$	h/b
Case 1	1000	5.00	4000	7.071	4
Case 2	1250	6.25	5000	7.071	4
Case 3	1400	7.00	5600	7.071	4

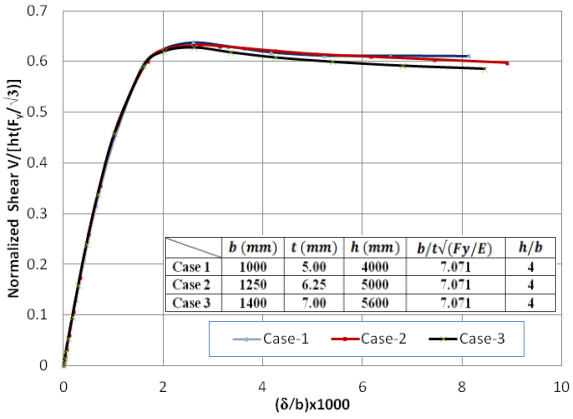

	b (mm)	t (mm)	h (mm)	$b/t\sqrt{(Fy/E)}$	h/b
Case 1	1000	5.00	4000	7.071	4
Case 2	1250	6.25	5000	7.071	4
Case 3	1400	7.00	5600	7.071	4

Figure 3 shows the applied shear versus the vertical drift for the three cases. These plots are different as the scale of fundamental parameters, the shear and the vertical drift are not dimensionless. However, the normalized applied shear versus normalized drift plots are identical. Therefore, it can be concluded that the change of scale does not affect the non-dimensionalized response, if the analysis models have the same dimensionless parameters.

A detailed parametric study established the ultimate shear capacity of the industrial duct side plate panels. An yield strength of $F_y = 250MPa$ and the modulus of elasticity $E = 200000MPa$ were used for this study. The plate slenderness b/t for the side plate panels considered were from 125 to 350 in steps of 25. The corresponding dimensionless parameters $b/t\sqrt{F_y/E}$, (and the dimensionless parameters Δ/t and σ_m/F_y corresponding to first yield due to internal pressure), were 4.419(0.86,0.88), 5.303(1.13,0.1), 6.187(1.38,0.117), 7.7071(1.65,0.127), 7.955(1.91,0.136), 8.839(2.17,0.141), 9.723(2.42,0.146), 10.607(2.67,0.151), 11.490(2.91,0.154) and 12.374(3.15,0.158). Investigation of the aspect ratio h/b of the practical duct reveals that its range is approximately from 2 to 10. Each of the plate satisfying the above parametric values were analyzed for ultimate loads and the shear load V versus in plane drift δ

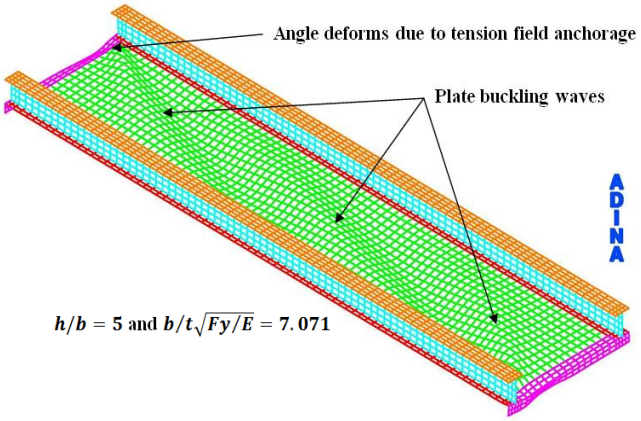

Figure 4: Deformed Shape of the Model

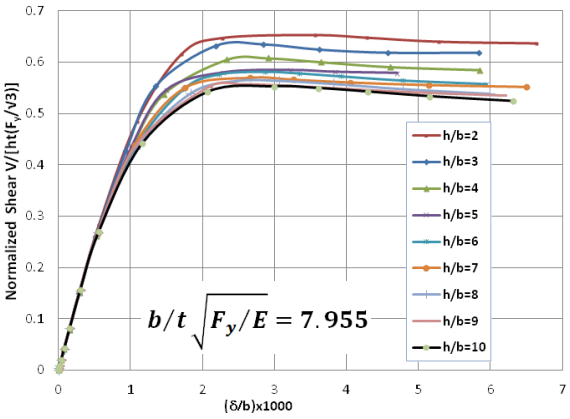

Figure 5: Normalized Shear versus Drift

history of each analysis was obtained. For each analysis model, the load versus drift history was converted into dimensionless form of normalized shear $V/[ht(Fy/\sqrt{3})]$ versus normalized drift δ/b history. A representative deformed shape of the side plate panel with $b/t\sqrt{F_y/E} = 7.071$ and $h/b = 5$, at the peak shear load, is shown in Figure 4. Figure 5 shows the normalized shear versus normalized drift history plots of the side plate panels with

Figure 3: Shear Vs drift relations and Normalized shear Vs Normalized drift relations

$b/t\sqrt{F_y/E} = 7.955$ and the various aspect ratios h/b under consideration. For each panel aspect ratio, the slope of the linear portion of the responses represents a non-dimensional stiffness. The initial non-dimensional stiffnesses were same. As the aspect ratio increases, the predicted normalized ultimate shear strength decreases slightly. It was observed that increasing number of bands of tension fields developed as the aspect ratio h/b increases from 2 to 10. It was also observed that the angles of the tension field within the stiffeners are the same. However, the top and bottom tension fields incline towards the intersection of the angle and the stiffener. This is because the boundary members should have enough flexural stiffness to anchor the tension fields. The low flexural stiffness of the angles at top and bottom of side panel does not provide enough rigidity to anchor the tension fields, and in the process angles experience local deformations, as shown in Figure 4.

From the normalized shear versus normalized drift history plots the normalized ultimate shear capacity $Vu/[ht(Fy/\sqrt{3})]$ of all the plates under consideration were extracted. In order to understand the influence of various parameters on the ultimate normalized shear strengths of duct side panels, the variation of $Vu/[ht(Fy/\sqrt{3})]$ with respect to $b/t\sqrt{F_y/E}$ and h/b were plotted in a three-dimensional representation. It was observed that the plate slenderness $b/t\sqrt{F_y/E}$ dominants the normalized ultimate

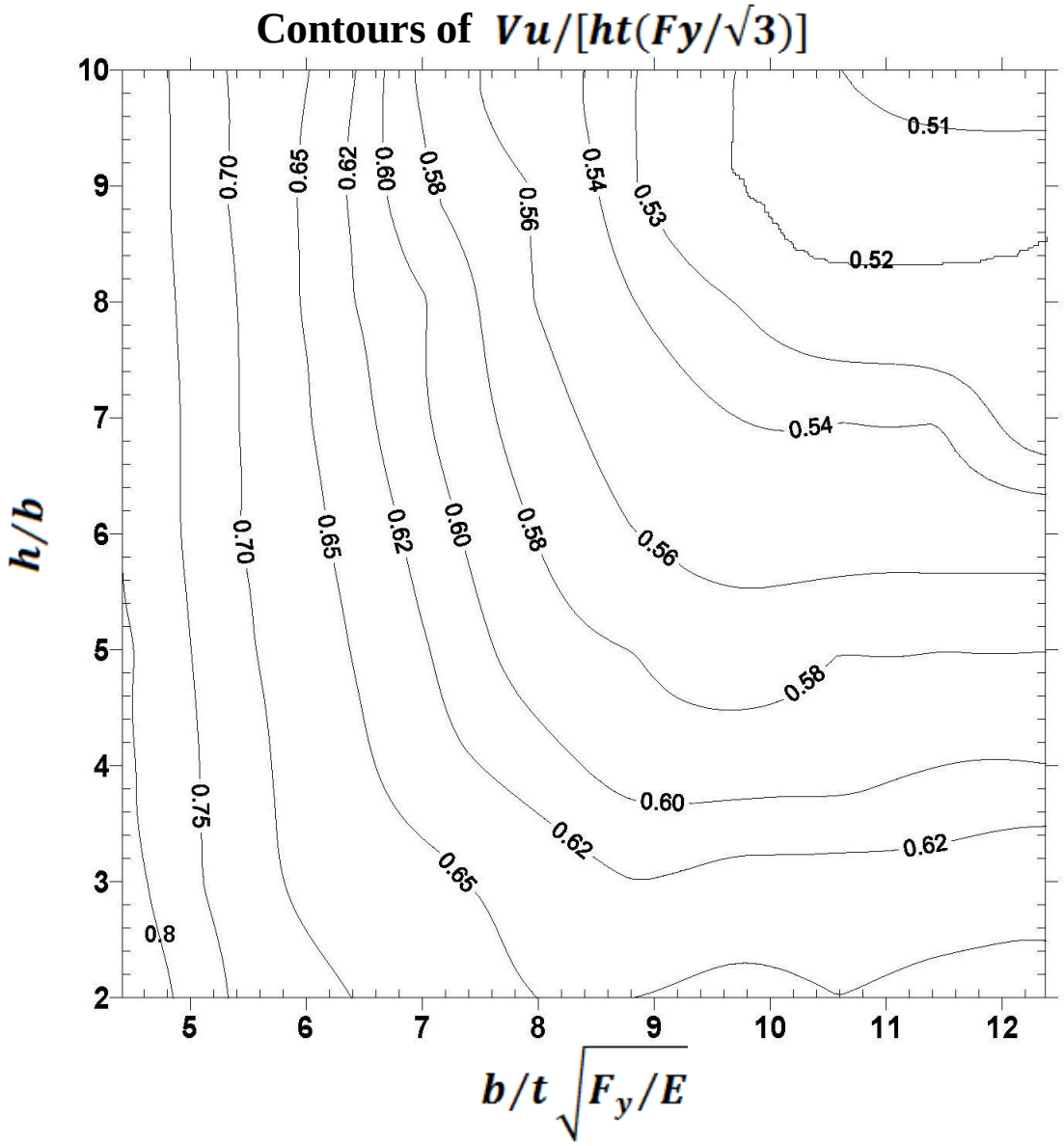

shear strength when its value is less than about 6. In this range, the aspect ratios h/b seem to have a

Figure 6: Contour of Normalized Ultimate Shear versus Dimensionless Parameters

minimal effect. However, for side plate panels with plate slenderness more than 6 (i.e. slender plates), the ultimate shear strength depends on both, aspect ratio h/b, and the plate slenderness $b/t\sqrt{F_y/E}$. Although the three-dimensional graphs provide the general pattern how the normalized shear strength is influenced by dimensionless parameters, establishment of contours of $Vu/[ht(Fy/\sqrt{3})]$ with respect to parameters $b/t\sqrt{F_y/E}$ and h/b might be more useful for design engineers. With this in mind, Figure 6, shows the contours of normalized ultimate shear strengths, which indicates that the shear strength of stockier plates, represented by $b/t\sqrt{F_y/E} < 6$, does not depend on the plate aspect ratio, and that those plates can carry more than 65% of shear yield strength concurrently with the internal pressures. On the other hand, the aspect ratio seems to influence the normalized ultimate shear strength of slender plates, defined here as $b/t\sqrt{F_y/E} > 6$. Figure 6 shows normalized ultimate shear strengths contours up to a value of 50% of shear yield strength $Vu/\left[ht\left(Fy/\sqrt{3}\right)\right] \approx 0.5$

5. Concluding Remarks

The ultimate shear resistance V_u of the slender side plate panels of large rectangular industrial ducts consists of plate shear buckling strength and the post-buckling strength due to tension field action. However, hitherto, the impact of internal pressure on the shear strength had not been investigated. Furthermore, higher aspect ratio of such plate panels may result in several bands of tension fields, which may provide additional contribution to the post-buckling strength. A finite element model of a duct side panel consisting of a plate panel bounded by two adjacent stiffeners and the corner angles at its top and bottom was built and verified. The model included initial geometrical imperfection, and realistic material models associated with structural steels. The out-of-plane deflections and the diaphragm stresses due to internal pressures, established in a previous study (Thanga, et al., 2013), was incorporated into the analysis model to account the effects of lateral pressures on the shear capacity of end panels. In this study, firstly, the dimensionless parameters affecting the behaviour of the side panel subjected to shear were identified and relevant non-dimensional parameters were derived. A parametric study was conducted for all the practical range of the these dimensionless parameters. For designers convenience, the contours of normalized ultimate shear strengths were established, which indicate that the shear capacity of stockier end panels $b/t\sqrt{F_y/E} < 6,$ depend on the slenderness rather than the aspect ratio, and the associated capacity is more than 65% of the corresponding shear yield resistance. The aspect ratio influences the ultimate shear strength of slender end panels of a rectangular industrial duct.

6. References

ADINA , (2009), ADINA 8.5 user manual, ADINA R & D Inc, Watertown, MA, USA.

AISC ASD, (1963), "Manual of Steel Construction- Allowable Stress Design" American Institute of Steel Construction ,Chicago.

AISC LRFD, (2005), "Manual of Steel Construction- Load and Resistance Factor Design." American Institute of Steel Construction, Chicago.

Basler, K. (1961), "Strength of Plate Girders in Shear." Journal of the Structural Division, In Proceedings of the American Society of Civil Engineers 87 (ST7), 151-180.

Langhaar, H.L., (1951), "Dimensional Analysis and Theory of Models." John Wiley, N.Y

Paik, K. J., Thayamballi, A.K., (2003), "Ultimate Limit State Design of Steel-Plated Structures." Wiley, Edition 1.

Timoshenko, S. P., Gere, J. M., (1961), "Theory of Elastic Stability." 2nd Edition. McGraw-Hill, New York.

Thanga,T., Sivakumaran,K.S., and Halabieh,B., (2013), "Stiffened Plates of Rectangular Industrial Ducts", Canadian Journal of Civil Engineering, Vol. 40, No. 4 : pp. 334-342 (April, 2013).